# Dose Rate Effects on Radiolytic Synthesis of Gold−Silver Bimetallic Clusters in Solution

**M. Treguer, C. de Cointet, H. Remita, J. Khatouri, M. Mostafavi, J. Amblard, and J. Belloni***

*Laboratoire de Physico-Chimie des Rayonnements (Associé au CNRS), Université Paris-Sud, 91405 Orsay Cedex, France*

**R. de Keyzer**

*Agfa-Gevaert N.V., B-2640 Mortsel, Belgium*

*Received: March 12, 1998*

Radiolysis of mixed $Au^{III}/Ag^{I}$ solutions at different dose rates is examined. The progressive evolution with dose of the UV−visible absorption spectra of radiation-induced metal clusters is discussed and compared with those calculated by Mie theory. The clusters have been also observed by transmission electron microscopy and analyzed by X-ray microanalysis and diffraction. At low dose rate, reduced silver atoms transfer an electron to gold ions (either free or at the surface of aggregates). Then, when $Au^{III}$ ions are totally reduced, reduction of the silver ions occurs in a second step at the surface of gold clusters, and silver-coated gold aggregates are obtained. At high dose rate, the shape of the absorption spectrum does not change with an increase in the absorbed dose and X-ray microdiffraction confirms that bimetallic alloyed Ag/Au clusters are synthesized. These results imply the preponderant influence of kinetics in the competition between the reduction−coalescence processes and intermetallic electron transfer. The segregation or the alloying of the metals is controlled by the reduction rate; a fast total reduction of both types of metal ions prevents the redox equilibrium through electron transfer from being established. A perfectly ordered nanocrystal, as observed by electron microdiffraction, also implies an intimate association of metal atoms from the early steps of reduction and aggregation.

## Introduction

For more than a decade[1−4] the radiation-induced generation of metal clusters has been proved to be a powerful method to synthesize at room temperature homodisperse nanocolloids and to control their size. Their efficiency, e.g., in catalysis, has been well recognized.[1,5−11]

Owing to their remarkable efficiency in catalysis,[12,13] the greatest interest is payed to bimetallic clusters where two metals are intimately alloyed. In particular cases, it has been found that $\gamma$ irradiation of a mixed solution of the ionic precursors of two metal elements could yield perfectly ordered bimetallic clusters characterized by electron diffraction.[7] The superlattice of the resulting bimetallic crystal particle depends on the ratio of ionic precursors; the structures CuPd and $Cu_3Pd$,[7−9] NiPt,[8,9] CuAu, and $Cu_3Au$[8,9] have been found. Recently, SnAu [14] was prepared and bimetallic alloyed AgPt [15] and AgPd [16] clusters with variable proportions have been characterized by optical absorption spectra. In the last example, the wavelength of the maximum of the surface plasmon band depends on the proportion in $Ag_xPd_{1-x}$ according to the Mie model for alloys. Alloyed AgPt clusters in ethylene glycol have been also prepared by chemical reduction of silver bis(oxalato)platinate and characterized by a homogeneous (111) lattice spacing.[17] Although the properties of both metals may be somewhat different, particularly with respect to redox reactions that control their formation through reduction, the alloying under irradiation was assigned[18] to the fast association between atoms or clusters and excess ions, which in the case of mixed solutions yield bimetallic complexes, reproducing more or less the probability of encounter (i.e., the composition of the initial ion mixture). Alternate adsorptions of one of the excess ions and further reductions of the complex by radiolytic radicals progressively build the alloyed cluster.

However, for numerous other couples of metal ions, the radiation-induced reduction of mixed ions does not produce eventually solid solutions but a segregation of the metals in a core/shell structure, such as for the case of Ag/Cu [19] (Ag in the core, Cu in the shell) or of Au/Pt.[15] In the last example, the more noble metal, Au, of the couple is reduced first to completion, and the second, Pt, is only reduced in a further step mostly at the surface of the previous clusters acting as nuclei.[20] The absorption spectrum changes in all these systems from the surface plasmon spectrum of the pure first metal to that of the last metal, suggesting that the latter is coated on the clusters formed first. Since both ions have almost the same initial probabilities of encountering the radiolytic reducing radicals and of being reduced, the results were interpreted as a consequence of an electron transfer from the less noble metal, as soon as it is reduced to one of its lower valency states, to the ions of the more noble metal, which is obviously favored by this displacement and reduced first.[7,15,19] The role of nuclei played by more noble metals such as Pt, Pd, or Cu is efficient to reduce the metal ions of Ni, Co, Fe, Pb, and Hg, which otherwise do not easily yield stable monometallic clusters through irradiation.[7−9] The bimetallic character of Fe/Cu clusters is attested by their ferromagnetic properties and the change of the optical spectrum relative to pure copper clusters.

S1089-5647(98)01467-9 CCC: $15.00 
Published on Web 05/14/1998

In a similar way, a photochemical method was used for preparing a bilayered Ag−Au composite by exposure to light at 253.7 nm of mixed $AgClO_4/HAuCl_4$ solutions in the presence of sodium arginate, the core being composed of gold and the shell of a silver-rich layer.[21] Similarly, a chemical reduction of a mixture of two ions among $Au^{III}$, $Pt^{IV}$, and $Pd^{II}$ (with decreasing order of redox potentials) yields bilayered clusters of Au/Pd, Au/Pt, or Pt/Pd.[22] Composite clusters of Ag/Pd have been also characterized.[23,24] Bilayered Au/Pt, Ag/Pt, and Ag/Au supported on imegolite fibers have been studied by optical absorption.[25]

Composite clusters have been also synthesized by the method of successive metal layer reduction.[26] Reduction of $Tl^+$,[27] $Au(CN)_2^-$,[28] $Pb^{2+}$,[29] $Cu^{2+}$,[19] $In^{3+}$, [29] or $Cd^{2+}$,[30] solutions in the presence of silver clusters leads to bilayered Ag/Tl clusters (thallium-coated silver), Ag/Au, Ag/Pb, Ag/Cu, Ag/In, or Ag/Cd, respectively. Similarly, the radiolytic reduction of $Pb^{2+}$,[31] $Cd^{2+}$, or $Tl^+$ [32] solutions in the presence of gold colloidal particles leads to bilayered Au/Pb, Au/Cd, or Au/Tl, respectively. An external shell of silver has been reduced in a second step at the surface of gold or palladium clusters, yielding Au/Ag [26] or Pd/Ag.[33] In some cases, a comparison between experimental spectra and calculated ones according to the Mie model for core−shell structures have shown that the plasmon absorption bands coincide rather well.[26] But in the case of gold-coated silver particles,[28] a recent discussion[34] concludes that the red shift observed by increasing the deposition of gold on preformed silver clusters corresponds better to the spectra predicted by the Mie model for spontaneous alloying that is supposed to occur through further diffusion of the atoms.

In the systems quoted above the more noble metal constitutes the core of the composite bilayered cluster owing to intermetallic electron transfer. Actually, it was shown by pulse radiolysis of a mixed solution of $Cu^{2+}$ (or $Ni^{2+}$) and $Ag^+$ that pure silver clusters are formed first because monovalent copper[35] or nickel[36] transfer electrons to silver ions. The displacement has been observed in pulse radiolysis experiments through the transient formation of a bimetallic complex such as $(AgCo)^{2+}$, associating atoms of one metal with ions of the second and then transferring an electron to another $Ag^+$.[37,38]

The same displacement may occur whenever metal clusters are in the presence of ions of another, more noble metal. Thus, zerovalent copper[39] and nickel[40] transfer readily electrons to more noble ions $Ag^+$, $Pd^{2+}$, and $AuCl_4^-$, which are thus reduced to clusters. The intermetallic electron transfer reaction is stoichiometrical; it has even been used to analyze quantitatively pure copper or nickel clusters after their formation through addition of silver ions and by measuring the optical absorption of the silver clusters. Note that $Pd^{2+}$ is reduced by preexisting copper clusters whereas the simultaneous reduction of mixed solutions of $Pd^{2+}/Cu^{2+}$ yields an alloy.[7−9]

The reduction of a mixture of ions, mostly plurivalent, implies a multistep process involving successive lower valency states of both elements also with possible disproportionations. The respective monoelectronic redox potentials of most of them still remain unknown so that a priori predictions on alloying or segregation of a couple of metals is not easy.

In fact, a recent pulse radiolysis study of a mixed system of monovalent cyanosilver and gold ions[41] has provided the first time-resolved observation of an intermetallic displacement. It is slow because it is controlled by the irreversible desorption toward the bulk of the ion released after reoxidation. The consequence is that the possible formation of a bimetallic cluster or the segregation of metals in a core/shell structure would depend on the competition between, on one hand, the irreversible release of the metal ions displaced by the excess ions of the more noble metal after electron transfer and, on the other hand, the radiation-induced reduction of both metal ions, which depends on the experimental conditions of dose rate. Complete reduction of both metal ions prevents any further intermetallic electron transfer. The aim of the present work is to describe an example of a bimetallic ionic system submitted to various dose rates of irradiation and to study the influence of the competition of the reduction rate versus electron-transfer rate on metal alloying. The clusters will be characterized by their optical absorption spectrum. However, this property is very sensitive to the cluster size and environment (stabilizer, pH). Thus, the alloyed or bilayered character of bimetallic clusters cannot be concluded from a simple comparison between spectra calculated from theoretical models and experimental ones. On the other hand, the final spectra in both cases are expected in close regions. Therefore, these data must be completed by the shift study of the spectrum at increasing reduction ratio, thus dose, and by independent investigations such as electron microscopy and diffraction and local X-ray microanalysis. The choice of the couple silver and gold was made because of the specific features of their surface plasmon optical spectra, both of which present an intense absorption band in the visible at quite distinct wavelengths (around 400 and 520 nm, respectively), because of the large amount of information available on monometallic silver clusters and to a lesser extent on gold clusters and optical data of gold−silver bulk alloys, and because of their catalytic properties in photographic processes.

## Experimental Section

The metal colloids were prepared in aqueous solution with 0.2 mol $L^{-1}$ 2-propanol (Prolabo) added as an $OH^\bullet$ and $H^\bullet$ scavenger and 0.1 mol $L^{-1}$ poly(vinyl alcohol) (PVA, MW of 86 000) (Aldrich) or poly(acrylic acid) (PAA, MW of 2000) (Aldrich) added as surfactants. The metal salts are, respectively, $Ag_2SO_4$ (Fluka) and $KAuCl_4$ (CLAL) in basic medium. The pH was adjusted to 10 with $NH_4OH$ (Prolabo). A few experiments were also done with $KAg(CN)_2$ and $KAu(CN)_2$ (CLAL).

The $\gamma$-irradiation sources were a $^{137}Cs$ $\gamma$ facility of 2000 Ci (Curie Institute, Orsay) and a $^{60}Co$ $\gamma$ facility of 9000 Ci (PAGURE, CE Saclay). The maximum dose rates used were 3.8 and 35 kGy $h^{-1}$, respectively. Other irradiation experiments were performed with a 20 kW and 10 MeV electron accelerator (CARIC Society) delivering trains of 14 $\mu$s (10−350 Hz) pulses through a scanning beam (1−10 Hz) of mean dose rate 2.2 kGy $s^{-1}$ (or 7.9 MGy $h^{-1}$ ).

The metallic solutions were $10^{-3}$ mol $L^{-1}$ for the total concentration of metal ions. Owing to the possible coexistence in solution of $Cl^-$ anions, arising from chloroauric ions reduction, and of $Ag^+$ cations, the bimetallic solutions to be irradiated were prepared by successive addition to the basic polymeric solution of first the $KAuCl_4$ solution and then the $Ag_2SO_4$ diluted solution. In the presence of PVA no turbidity caused by AgCl colloid formation was observed. Solutions were thoroughly deaerated by bubbling $N_2$ gas. The solutions were stored in the dark as soon as prepared and also irradiated once. After irradiation the solutions remained perfectly limpid.

The primary effects of the interaction of high-energy radiation such as particle beams and X-ray or $\gamma$ photons with a solution of metal ions are the excitation and the ionization of the solvent. Fast subsequent processes, dissociation of excited states, ion−molecule reaction, and radical−radical recombination lead

rapidly to molecular and radical species able to react with the dilute solute. For example, in aqueous solution

$$H_2O \rightsquigarrow H_2O^*, H_2O^+, e^- \rightarrow e^-_{aq}, H_3O^+, H^\bullet, OH^\bullet, H_2, H_2O_2 \quad (1)$$

$H^\bullet$ atoms and solvated electrons $e^-_{aq}$ are strong reducing agents capable of reducing metal ions to lower valencies and finally to metal atoms. Reverse oxidation by $OH^\bullet$ radicals is avoided by addition of radical scavengers such as an alcohol. Isopropyl alcohol yields by reaction with $OH^\bullet$ and $H^\bullet$ a secondary radical $(CH_3)_2C^\bullet OH$ that also could efficiently reduce the metal ions $M^+$ when adsorbed on clusters

$$(CH_3)_2CHOH + OH^\bullet (H^\bullet) \rightarrow (CH_3)_2C^\bullet OH + H_2O (H_2) \quad (2)$$

$$e^-_{aq} + M^+ \rightarrow M^0 \quad (3)$$

$$(CH_3)_2C^\bullet OH + M^+ \rightarrow (CH_3)_2CO + M^0 + H^+ \quad (4)$$

Under basic conditions the protons are readily neutralized. Then starts the association of atoms, with excess ions either of the same metal or of the second metal, and the coalescence of atoms into clusters of increasing nuclearity.

Samples for transmission electron microscopy (TEM) and electron diffraction were prepared in a glovebox flushed with $N_2$ by deposition of droplets of irradiated solutions diluted 20 times onto copper grids coated with amorphous carbon membrane (10−30 nm thick) and by drying under $N_2$. JEOL microscopes of type JEM 100 CX II are used currently at 100 kV voltage. One is equipped with a LINK analysis system of type AN 10000, allowing X-ray spectroscopy experiments to be performed. This local X-ray microanalysis enables us to determine the element content of each particle. The detector is a 30 $mm^2$ Si (Li) diode with an ultrathin window allowing the identification of light elements (B, C, O).

## Results

**$\gamma$ Irradiation at Low Dose Rate (0.25−3.8 kGy $h^{-1}$).** *Optical Properties*. It is well-known that the surface plasmon spectrum of metal nanocolloids is highly dependent on the environment: ion concentration, surfactant, pH, etc. For that reason, spectra of monometallic solutions of each of the metal ions have been recorded after irradiation under the same conditions as for irradiated mixed solutions. The final spectra of irradiated monometallic $KAuCl_4$ or $Ag_2SO_4$ solutions ($5 \times 10^{-4}$ mol $L^{-1}$ in metal ion) are shown in the inset of Figure 1a. Under these conditions, the silver cluster band at complete reduction is centered at 400 nm with an extinction coefficient per atom $\epsilon_{400}(Ag_{n,PVA})$ of 13 000 L $mol^{-1}$ $cm^{-1}$ and 130 nm of bandwidth at half-height. The absorbance $OD_{max}$ increases linearly with the dose, and the radiolytic yield is $G = 6$ atoms per 100 eV absorbed (corresponding to the total scavenging of $e^-_{aq}$ and $(CH_3)_2C^\bullet OH$ radicals). The spectrum of the irradiated monometallic $KAuCl_4$/PVA solution is a broad surface plasmon band centered at 520 nm with an extinction coefficient per atom of $\epsilon_{520}(Au_{n,PVA}) = 2700$ L $mol^{-1}$ $cm^{-1}$ (inset, Figure 1a). The band shape and intensity are very similar to those of dilute solutions. The mean radiolytic yield of $Au^{III}$ reduction to $Au^0$ is $G = 2$ atom/100 eV ($G = 6$ red. equiv/100 eV) even though the yield is smaller for a short period at very low doses.

Figures 1a and 2 present the time evolution of the optical absorption spectra of mixed solutions of $KAuCl_4$ and $Ag_2SO_4$ irradiated in the presence of PVA at dose rates of 0.25 and 3.8 kGy $h^{-1}$, respectively. The optical absorption spectrum is first identical to that of pure gold clusters with a maximum at 520 nm up to a dose of 2 kGy as shown in Figure 2. At that dose about 80% of gold ions are reduced. Then the intensity continues to increase but the single absorption maximum progressively shifts to the blue and the colloidal solution turns from pink to deep yellow. At a dose rate of 0.25 kGy $h^{-1}$ and at doses higher than 5 kGy, the spectra present two bands at 410 and 490 nm. The final spectrum in Figure 1 is different from that of a mixture of separate, coexisting monometallic clusters of gold and silver without any interaction. The spectrum would be in that case a sum of the two components as shown

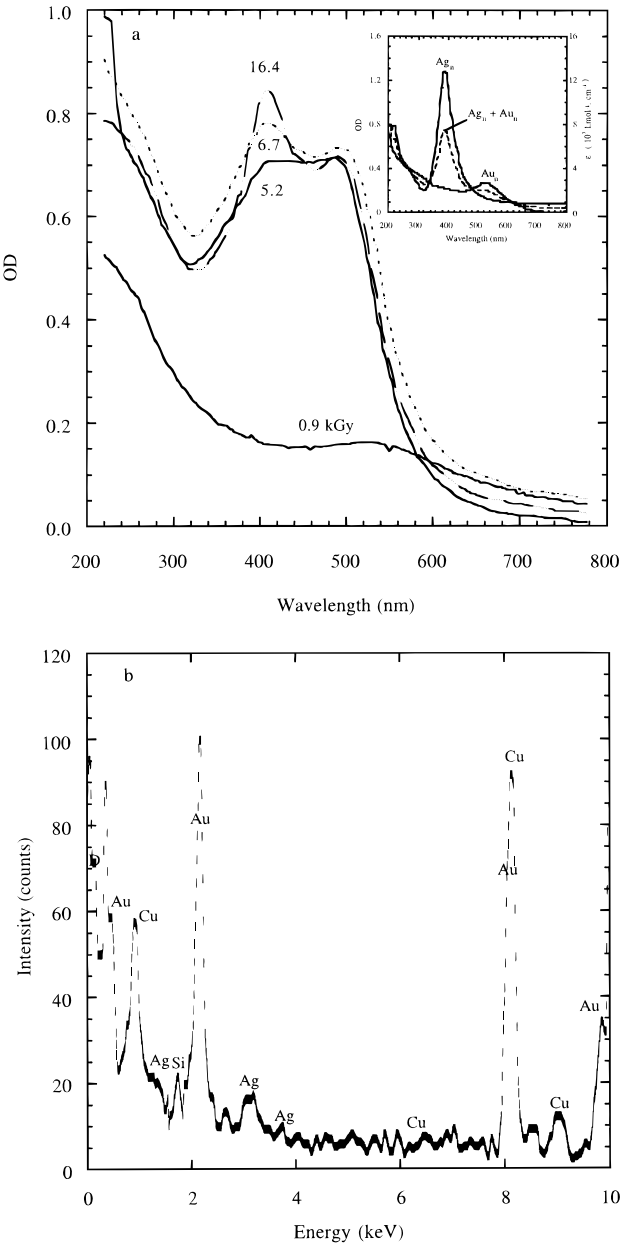


**Figure 1.** (a) Evolution with increasing dose of the absorption spectra of a mixed solution of $Au^{III}/Ag^I$ (50/50) irradiated at a dose rate of 0.25 kGy $h^{-1}$: $[Au^{III}] = [Ag^I] = 5 \times 10^{-4}$ mol $L^{-1}$, [PVA] = 0.1 mol $L^{-1}$, [2-propanol] = 0.2 mol $L^{-1}$, pH = 10; room temperature. Optical path = 0.2 cm. (Inset, −) Optical absorption spectra of pure silver or gold colloids stabilized by PVA in aqueous solutions: $[Au^{III}]$ or $[Ag^I]$ $= 5 \times 10^{-4}$ mol $L^{-1}$, [PVA] = 0.1 mol $L^{-1}$, [2-propanol] = 0.2 mol $L^{-1}$, pH = 10; dose = 20 kGy. (Inset, - - -) Calculated absorption spectrum assuming a mixture of coexisting pure $Ag_n$ and $Au_n$ clusters. (b) Local X-ray microanalysis of clusters obtained under the same conditions as above with a dose of 0.8 kGy.

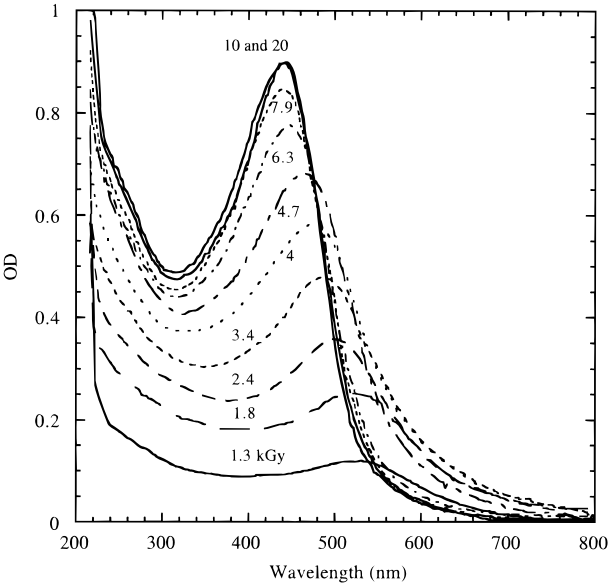


**Figure 2.** Evolution with increasing dose of the absorption spectra of a mixed solution of $Au^{III}/Ag^{I}$ (50/50) irradiated at a dose rate of 3.8 kGy $h^{-1}$: $[Au^{III}] = [Ag^{I}] = 5 \times 10^{-4}$ mol $L^{-1}$, [PVA] = 0.1 mol $L^{-1}$, [2-propanol] = 0.2 mol $L^{-1}$, pH = 10. Optical path = 0.2 cm.

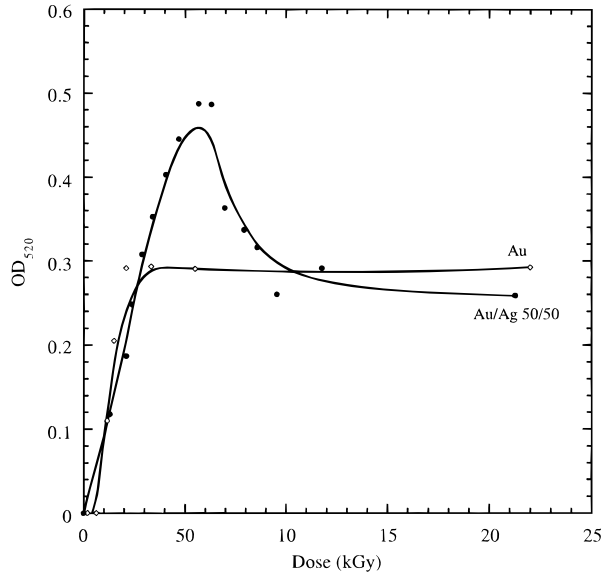


**Figure 3.** Evolution with increasing dose of the optical density at $\lambda$ = 520 nm at a dose rate of 3.8 kGy $h^{-1}$ for pure $Au^{III} = 10^{-3}$ mol $L^{-1}$ solution or a mixed $Au^{III}/Ag^{I}$ (50/50) solution with total metal concentration of $10^{-3}$ mol $L^{-1}$: [PVA] = 0.1 mol $L^{-1}$, [2-propanol] = 0.2 mol $L^{-1}$, pH = 10. Optical path = 0.2 cm.

in the inset of Figure 1, characterized by two distinct maxima at 400 and 520 nm.

At a dose rate of 3.8 kGy $h^{-1}$ the final spectrum presents a maximum at 440 nm, a value which is still higher than that of pure silver clusters at 400 nm under the same experimental conditions (inset, Figure 1a). In the low-dose region (<0.7 kGy) the absorbance increase is close to that of a pure gold solution ($5 \times 10^{-4}$ mol $L^{-1}$) with the same yield as if silver ions would not compete at all with gold ions for the scavenging of radiolytic reducing species (Figure 3). Nonetheless, the values of the scavenging rate constants of $e^{-}_{aq}$ by silver and gold ions are close. This suggests that the reduced silver atoms undergo in a further step a reverse oxidation through electron transfer to gold ions (gold is a more noble metal than silver in the presence of chloride). Therefore, $Ag^{+}$ ions act essentially as an electron

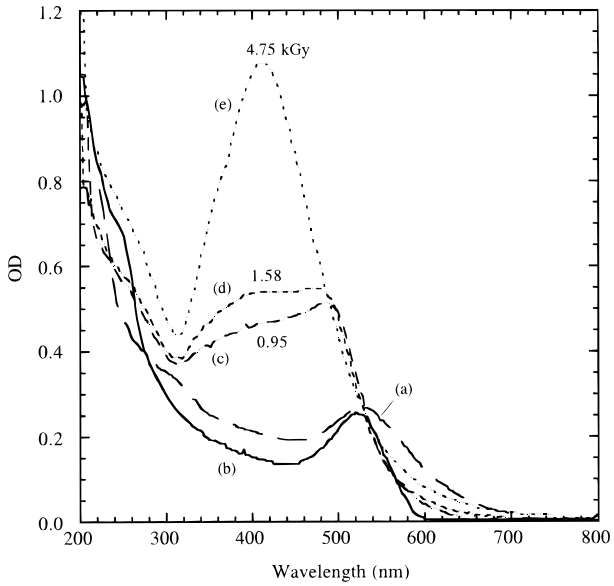


**Figure 4.** Absorption spectra of (a) gold aggregates obtained by irradiation of a solution of $[Au^{III}] = 5 \times 10^{-4}$ mol $L^{-1}$, [PVA] = 0.1 mol $L^{-1}$ (dose rate: 3.8 kGy $h^{-1}$; dose: 1.8 kGy). (b) Solution containing gold colloids (solution a) and $[Ag^{I}] = 5 \times 10^{-4}$ mol $L^{-1}$ without further irradiation. (c, d, e) Irradiated solutions containing initially the colloidal gold solution (solution a) and $[Ag^{I}] = 5 \times 10^{-4}$ mol $L^{-1}$ with different additional doses: [2-propanol] = 0.2 mol $L^{-1}$, pH = 10, dose rate = 3.8 kGy $h^{-1}$. Optical path = 0.2 cm.

scavenger and also as an electron relay toward gold ions as long as gold ions are not almost totally reduced (Figure 2). The blue shift of the surface plasmon spectrum at doses higher than 2 kGy (Figures 1a and 2) indicates indeed that the cluster composition also changes when the dose increases from almost pure gold clusters (0−2 kGy) to clusters coated with an increasing layer of silver. Even though the final spectrum is not that of monometallic silver clusters, the maximum of the specific band of gold clusters has disappeared. In fact, the gold clusters formed at the early stage adsorb most of excess silver ions and when the dose increases, silver reduction occurs at the surface of gold particles. If a lot of $Ag^{+}$ are adsorbed, the probability in this dose range of reducing isolated silver ions and therefore of forming pure silver clusters is small. The reduction yield also decreases at higher doses because of the very small concentration of clusters (where the ions are fixed) and because of the favored competition of the biradical recombination of reducing species compared with their scavenging by charged clusters. It can be considered that all ions are reduced ($2 \times 10^{-3}$ equiv $L^{-1}$) at about 10 kGy (40 or 3 h irradiation, depending on the dose rate). The final intensity corresponds to a mean extinction coefficient per Ag or Au atom of $\epsilon_{440} = 4700$ L $mol^{-1}cm^{-1}$ (Figure 2). At high doses (>1 kGy) in Figure 3, the silver-coated gold clusters exhibit a lower extinction coefficient per Ag or Au atoms at 520 nm than pure gold clusters. The subcolloidal solutions are then stable with time, and their spectrum does not change, even in the presence of air.

To check the validity of the above mechanism of successive reduction of gold and silver ions, experiments were performed on the radiolytic reduction of $5 \times 10^{-4}$ mol $L^{-1}$ $Ag^{+}$ added *after* the end of the radiation-induced synthesis of gold clusters ($5 \times 10^{-4}$ mol $L^{-1}$ $Au^{0}$) (Figure 4). The surface plasmon band of $Au_n$ is slightly changed when $Ag^{+}$ ions are added (Figure 4b). The final spectrum is not so different from that obtained after the reduction of the mixture (Figure 2): $\lambda_{max} = 415$ nm and $\epsilon_{415} = 5500$ L $mol^{-1}$ $cm^{-1}$. However, a difference exists for intermediate doses. In Figure 4, the intermediate spectra

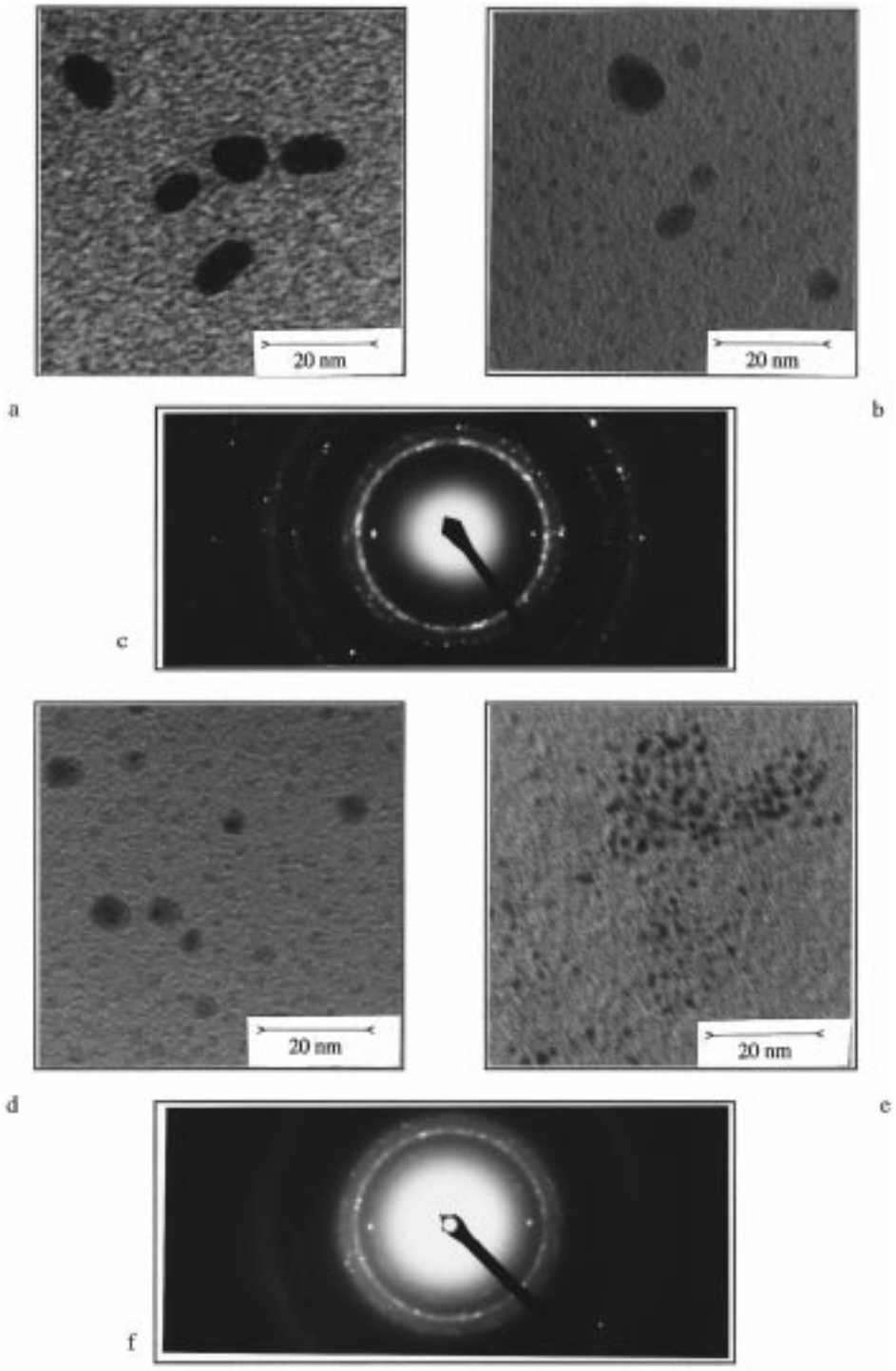


**Figure 5.** Micrographs (a, b, d, e) and electron diffraction pattern (c, f) of Ag/Au (50/50) and (32/68) bimetallic particles stabilized by PVA or PA and obtained at different dose rates: (a) dose rate = 0.25 kGy $h^{-1}$, dose = 20 kGy (PVA); (b) dose rate = 35 kGy $h^{-1}$, dose = 20 kGy (PVA); (c) diffractogram of the sample corresponding to micrograph in part b (note the presence of two central intense spots corresponding to the lattice distance $d_{110}$ due to the existence of a perfectly ordered alloy of $A_3B$ stoichiometry (A = Ag or Au)); (d) dose rate = 35 kGy $h^{-1}$, dose = 20 kGy (PA); (e) dose rate = $7.9 \times 10^3$ kGy $h^{-1}$, dose = 30 kGy (PVA); (f) diffractogram of a sample Ag/Au (32/68), dose rate = 35 kGy $h^{-1}$, dose = 20 kGy (PA).

correspond to layers of gold in the core and silver in the shell formed successively as in a previous work.[26] It seems that when both ions are initially present and irradiated together with a dose rate of 3.8 kGy $h^{-1}$, the transition between gold and silver reduction is less exclusive; in the intermediate dose region, gold and silver are more or less alloyed as if the electron transfer from Ag atoms to the last gold ions would be too slow and thus less efficient.

*Structural Investigations*. Electron micrographs taken from totally reduced sample indicate that the size distribution ranges from 1.5 to 12 nm with unimodal size distribution (Figure 5a). Local X-ray microanalysis of clusters obtained after partial reduction of a solution $Au^{III}/Ag^{I}$ (50/50) with a dose rate of 0.25 kGy $h^{-1}$ indicates clearly again that gold is predominant (Au/Ag = 90/10) in the particles at a dose of 0.8 kGy, which corresponds to a reduction of only 30% of ion equivalents

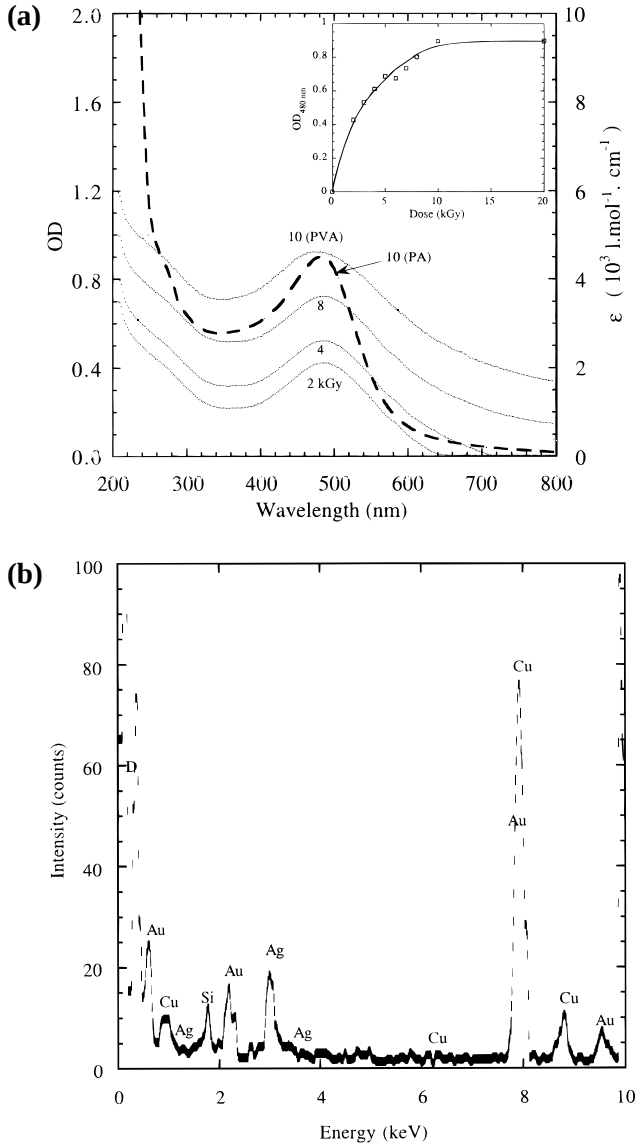


**Figure 6.** (a) Evolution with increasing dose of the absorption spectra of a mixed solution of $Au^{III}/Ag^{I}$ (50/50) irradiated at 35 kGy $h^{-1}$: $[Au^{III}] = [Ag^{I}] = 5 \times 10^{-4}$ mol $L^{-1}$, [PVA] = 0.1 mol $L^{-1}$, [2-propanol] = 0.2 mol $L^{-1}$, pH = 10; (dotted line) spectrum with [PA] = 0.1 mol $L^{-1}$ at pH 4.5 under the same conditions. Optical path = 0.2 cm. (Inset) Evolution with increasing dose of the optical density at $\lambda = 480$ nm. (b) X-ray analysis of Ag−Au (50/50) bimetallic particules stabilized by PVA $5 \times 10^{-2}$ mol $L^{-1}$ at a dose of 6.4 kGy.

(Figure 1b). This confirms the above interpretation of the synthesis of a core/shell structure under these conditions.

***γ* Irradiation at a Dose Rate of 35 kGy h$^{-1}$.** The above results imply that the displacement of silver atoms by gold ions occurs along the $\gamma$ irradiation in competition with the direct reduction of both ions by the radiolytic species. To accelerate the reduction with respect to the chemical reaction of metal displacement, the study has been repeated with the same systems at a higher dose rate, 35 kGy $h^{-1}$.

*Optical Properties*. Figure 6a presents the evolution of the optical absorption spectrum of a mixed solution at increasing doses. When mixed solutions of $KAuCl_4$ and $Ag_2SO_4$ are irradiated in the presence of PVA at a dose rate of 35 kGy $h^{-1}$, the shape of the spectrum does not change and the intensity progressively increases with the dose similarly for all the wavelengths. In contrast with the lower dose rate (Figures 1a and 2), all spectra present the same new band, centered at 480 nm, between those of the monometallic clusters (inset of Figure 1). The previous maxima of monometallic clusters are no longer observed. The absorbance at the maximum at complete reduction (20 kGy) corresponds to an extinction coefficient of $\epsilon_{480} = 4500$ L $mol^{-1}$ $cm^{-1}$ per metal atom. Note also that at this wavelength the extinction coefficients of both monometallic clusters have the same value (around 2000 L $mol^{-1}cm^{-1}$), which is much lower than for the bimetallic system. This identical spectrum shape at any dose therefore bears witness to the existence of the same strong interaction between the two metals that seemingly are alloyed in a constant proportion from the lowest doses and consequently identical to that of the ionic precursors. The particle size increases with dose, thus explaining the rise of a red component in the spectrum. From the initial slope of the absorbance increase with dose (inset, Figure 6a) and from $\epsilon_{480}$, we deduce a radiolytic yield close to $G = 6$ equiv/100 eV.

Experiments in the presence of the surfactant sodium polyacrylate (PA), instead of PVA, were conducted at pH 4.5. After complete reduction of $Au^{III}/Ag^{I}$ (50/50) solutions, the optical absorption spectrum is quite similar in position and intensity of the band compared with spectra with PVA, except that in the 600−800 nm domain the light scattering is much less important than with PVA (Figure 6a), suggesting that the mean size of clusters stabilized by PA is smaller as usually observed also for monometallic particles.[3]

*Structural Investigations*. The spectroscopic study at 35 kGy $h^{-1}$ strongly supports an intimate alloying of the metals. The following results must provide a local characterization of the particles. The micrographs obtained by TEM of clusters from mixed gold/silver 50/50 PVA solutions after irradiation (Figure 5b) show isolated clusters with a diameter of 2−3 nm, often linked as in a short chain, but also a few larger particles of 10−15 nm. Clusters prepared in the presence of PA (Figure 5d) are isolated and more homodispersed, and their mean size is smaller, 2−3 nm, than for PVA stabilized clusters. The corresponding spectrum in Figure 6a is narrower and does not contain the red component assigned to larger clusters. Small alloyed bimetallic Ag−Pt clusters were also formed when stabilized by PA.[15]

The methods able to give local information on a possible bimetallic character of clusters require generally larger objects. When the PVA is half as concentrated, the mean size of clusters becomes 20−25 nm and local X-ray analysis is easier to carry out. The X-ray analysis of a population of particles indicates an average composition of 50% of each of the elements Ag and Au (Figure 6b), identical to that of the precursors before irradiation. When it concerns a single particle of a large enough size for local analysis, the relative composition for the majority of clusters is also close to 50 ± 10%. However, some single particles or some groups of clusters exhibit more dissymmetric content, around 75/25% with one metal or the other being predominant. These results suggest, from the dose-independent spectra, that both types of metal atoms are intimately alloyed in the clusters.

Silver and gold crystallize with the same fcc lattice and very similar $a_o$ parameters (Ag, 0.4086 nm; Au, 0.4078 nm). Solid solutions might therefore easily form, and the random replacement of atoms of one element by atoms of another cannot generally be detected by electron diffraction analysis. However, if certain superlattices are preferred with a perfectly ordered arrangement of the two kinds of atoms, as already observed for $Cu_3Pd$ and CuPd,[7−9] $Cu_3Au$ and CuAu,[8,9] or NiPt,[8,9] the diffraction patterns are specific. In Figure 5c is shown the

pattern obtained with some clusters of a sample Ag−Au/PVA, analyzed on a single cluster. To the Debye−Scherrer diagram, which can be indexed as a Ag (or Au) fcc structure, are now superimposed two new intense spots corresponding to a distance $d_{110}$, which in a solid solution is usually absent. This clearly indicates a superlattice (Figure 5d) of a perfectly ordered alloy of stoichiometry $M_3M'$ with a long-distance order. However, the crystal parameters of Au and Ag are so similar that we cannot conclude whether the crystal is $Ag_3Au$ or $AgAu_3$. Note that some similar compositions have also been detected by the X-ray microanalysis. The electron diffraction results support the conclusion of an intimate mixture of both metals, and the alloyed character of the cluster is therefore established without ambiguity.

Similarly, X-ray diffraction observations have been performed on individual clusters prepared in the presence of PA by selecting rare objects with a size of around 10 nm. The diffraction patterns obtained, for example, on the sample formed in $Au^{III}/Ag^{I}$/PA 68/32 present for each of these clusters the characteristic spots corresponding to the distance $d_{110}$ and indicating the presence of the superlattices of $AgAu_3$ (Figure 5f).

The difference between the optical properties of gold−silver clusters prepared under the dose rate conditions of 3.8 or 35 kGy $h^{-1}$ is thus due to a negligible importance in the latter case of the reverse electron-transfer process from silver atoms (the less noble metal) to gold ions (the more noble metal in the present environment) relative to the rate of direct reduction of both ions by radiolytic entities. The process of the progressive building of alloyed clusters results essentially from coalescence between atoms and clusters, whatever the metal would be, and from the mixed association of atoms or clusters of one metal and the ions of the second followed by their reduction at the cluster surface.[18] The energetics of the mixed system are obviously not affected by the conditions of irradiation such as the dose rate, and differences between the redox properties of both metals still exist. However, the higher rate of reduction does not allow it to reach the corresponding redox equilibrium through intermetal electron transfer. Actually, coalescence, association with ions, and radiolytic reduction are occurring from the equilibrium concerning the mutual reactions between metals. When the radiolytic reduction has consumed all the ions, the displacement becomes excluded.

**Electron Beam Irradiation at High Dose Rate (7.9 MGy $h^{-1}$).** *Optical Properties.* To exclude any possible electron transfer and thus an enrichment of clusters in the more noble metal at the expense of a second metal, irradiation experiments have also been performed with a pulsed electron beam facility delivering a much higher dose rate of 7.9 MGy $h^{-1}$.

The dose effect on the radiolysis of the mixed solution (50/50) by the electron accelerator is shown in Figure 7. A dose close to 15 kGy suffices for the total reduction, and the maximum is at about 480 nm. The shape and the intensity of the absorption spectrum in the range 5−20 kGy are quite similar to that obtained by $\gamma$ irradiation at 35 kGy $h^{-1}$. The conclusions on silver−gold alloying derived at the latter dose rate still hold. For doses above 20 kGy, i.e., after complete reduction, the spectrum presents a slight blue shift of the maximum and an increasing component in the red, which indicates light scattering due to larger particles.

When solutions of variable proportions of silver and gold ions are irradiated with the same dose rate of 7.9 MGy $h^{-1}$, the spectrum shape is also in all cases independent of the dose up to the total reduction. However, the wavelength and the extinction coefficient of the maximum markedly depend on the relative initial concentrations of silver and gold ions (Figure 8). All solutions after complete reduction are stable even in the presence of air.

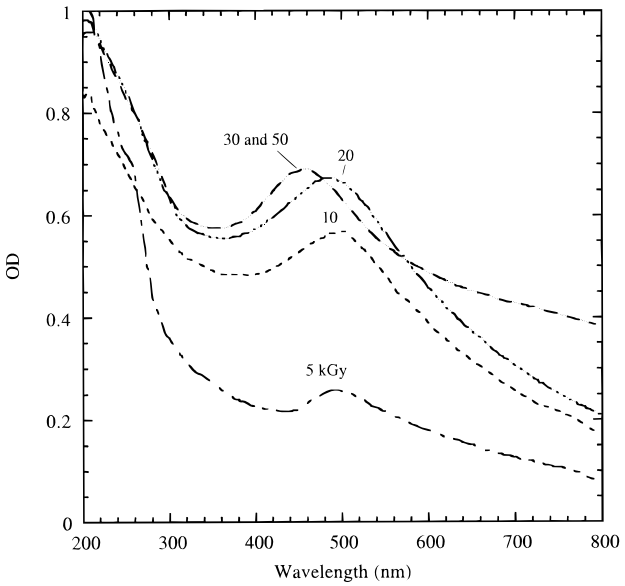


**Figure 7.** Absorption spectra at increasing dose of a mixed solution of $Au^{III}/Ag^{I}$ (50/50) irradiated by a pulsed electron beam (dose rate = 7.9 MGy $h^{-1}$): $[Au^{III}] = [Ag^{I}] = 5 \times 10^{-4}$ mol $L^{-1}$, [PVA] = 0.1 mol $L^{-1}$, [2-propanol] = 0.2 mol $L^{-1}$, pH = 10.

The favorable effect of high dose rate conditions to inhibit an intermetal electron transfer and to synthesize intimately alloyed clusters encouraged us to apply the same method to other systems. In particular we investigated the $Ag(CN)_2^-/Au(CN)_2^-$ solution where silver and gold metals induced by irradiation were clearly segregated in gold-coated silver clusters as shown previously.[41] In $\gamma$ radiolysis and even in pulse radiolysis with only partial reduction, silver atoms with more positive redox potential than gold were indeed formed first. However, when such a mixed solution is irradiated at a high dose rate as above (7.9 MGy $h^{-1}$) with a dose sufficient to reduce *all* the ions within a very short time, a new spectrum is found (Figure 9), distinct from the previous results.[41] The maximum is now at $\lambda_{max}$ = 420 nm, and the extinction coefficient per atom of Ag or Au is $\epsilon(AgAu)_{n,CN^-}$ = 2250 L mol $^{-1}$ $cm^{-1}$. These features favor the conclusion that the clusters formed are alloyed and that the segregation process due to the metal displacement is at least markedly prevented by a very fast quenching reduction. If the dose is less than required for the complete reduction, postirradiation displacement of gold by silver ions occurs readily and the spectrum observed is the silver band with the specific UV peaks of excess $Au(CN)_2^-$ ions.

Fast reduction through an intense, short electron irradiation does also allow even the deposit of reduced Au as an external shell on preformed $Ag_n$ (*less noble*). The silver clusters are produced first in a pure silver sulfate solution (Figure 10a). Then the $Au^{III}$ solution is mixed with the silver cluster sol. The spectrum evolution of the $Ag_n/Au^{III}$ system submitted to the electron beam irradiation immediately after mixing is now reversed relative to Figure 2, shifting from that of $Ag_n$ to a plasmon band of gold-coated silver with a maximum at 450 nm (Figure 10b). The final spectrum is similar to previous data on the same core/shell structure obtained after reduction of gold cyanide according to the expected order of silver coated by gold because in the presence of $CN^-$ gold was less noble than silver.[28]

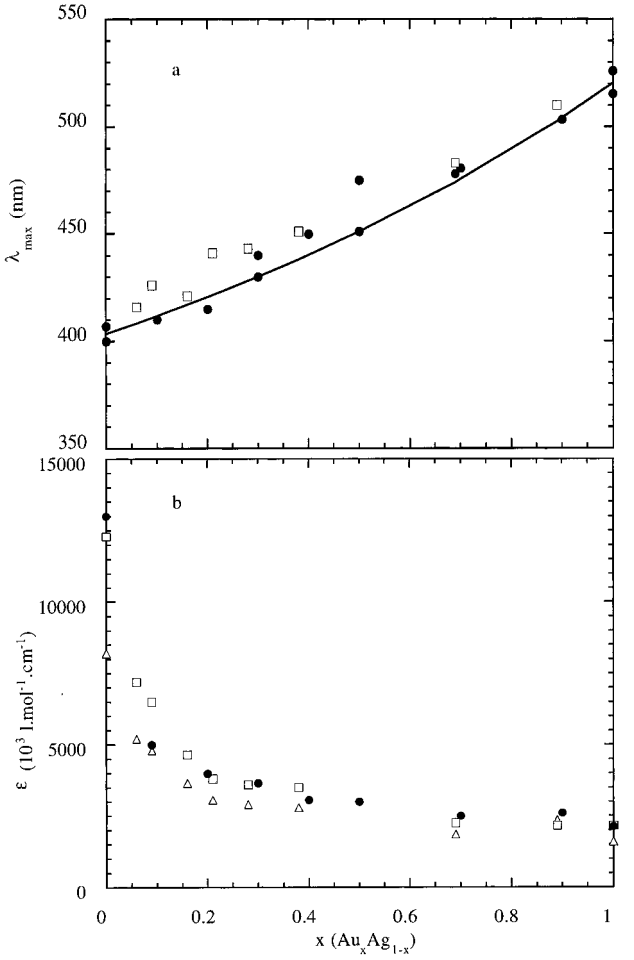


**Figure 8.** (a) Maximum wavelength of gold−silver plasmon band as a function of the mole fraction of gold at a dose rate of 7.9 MGy $h^{-1}$ and a dose of 20 kGy, where total metal concentration = $10^{-3}$ mol $L^{-1}$, [PVA] = 0.1 mol $L^{-1}$, 2-propanol = 0.2 mol $L^{-1}$: (●) experiments (this work); (□) calculated values by eq 5 with Ripken's optical data;[44] (−) eq 9. (b) Extinction coefficient at the maximum of the gold−silver plasmon band as a function of the mole fraction of gold: (●) experiments (this work); (□) eq 5 with $r$ = 5 nm; (△) eq 5 with $r$ = 3 nm.

Note that in the present experiments, in contrast, gold is more noble than silver and yet the inversion is made possible because of the sudden reduction of $Au^{III}$ in the second step. If gold ions are added at a higher concentration of $10^{-3}$ mol $L^{-1}$ and then the system is suddenly irradiated up to 20 kGy, the final spectrum is almost that of the surface plasmon band of pure gold clusters because the coating is now much thicker (Figure 10c).

*Electron Microscopy*. The TEM micrographs of the mono- and bimetallic samples (Figure 5e) prepared by electron beam irradiation (10 kGy) show that the clusters are particularly homodisperse and that the mean size is markedly smaller (<3 nm) than for $\gamma$-induced clusters. This may be due to a much higher concentration of single atoms suddenly produced in the solution, which act as many individual centers for ion association and further coalescence (in contrast with low dose rate irradiations where fewer nuclei adsorb excess ions then reduced in situ). At higher doses, the micrographs present an increasing number of clamps, as in Figure 5e, containing several small clusters and that could be formed by cross-linking of the polymer when all ions have been reduced. The local X-ray analysis of single particles has not been possible because of their very small size.

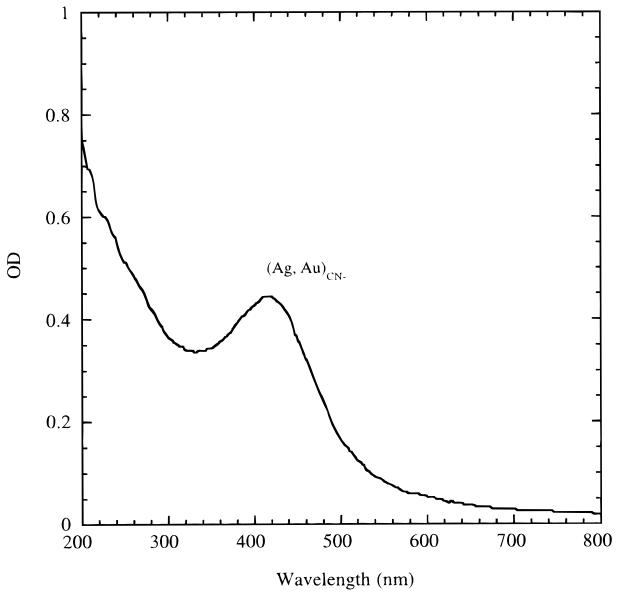


**Figure 9.** Absorption spectra of a mixed solution of $Au^I/Ag^I$ (50/50) in the presence of cyanide irradiated by a pulsed electron beam (dose rate = 7.9 MGy $h^{-1}$, dose = 10 kGy): $[Au^I] = [Ag^I] = 5 \times 10^{-4}$ mol $L^{-1}$, [PVA] = 0.1 mol $L^{-1}$, [2-PrOH] = 0.2 mol $L^{-1}$, pH = 10. Optical path = 0.2 cm.

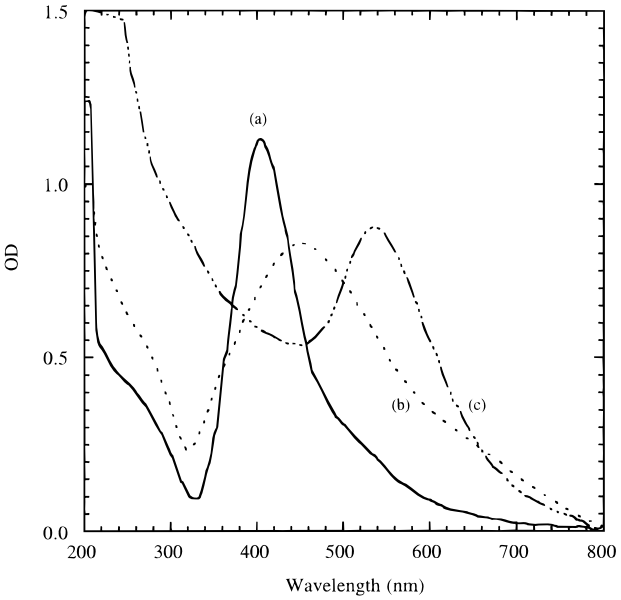


**Figure 10.** Absorption spectra of core/shell Au/Ag clusters induced by pulsed electron beam (dose rate = 7.9 MGy $h^{-1}$): (a) silver clusters prepared under conditions of inset of Figure 1; (b) solution of part a in the presence of $[Au^{III}] = 5 \times 10^{-4}$ mol $L^{-1}$ after irradiation with a dose of 10 kGy; (c) solution of part a with added $[Au^{III}] = 10^{-3}$ mol $L^{-1}$ after irradiation with 20 kGy. Optical path = 0.2 cm.

## Discussion

**Surface Plasmon Spectra of Bimetallic Clusters (Mie Model).** The above study of the dose effect on the shape evolution of the surface plasmon spectra of clusters produced from the progressive reduction of a metal ions mixture has demonstrated that the clusters were intimately alloyed or core/shell layered as a consequence of a competition between kinetics of the intermetallic electron tranfer and of the reduction controlled by the dose rate. It would be of interest to compare the spectra so clearly identified for both types of mixed cluster with the theoretical models.

The Mie model[42,43] has already been applied to various types of bilayered clusters[26,28,33,34] of *core/shell structure* consisting of one metal nucleus and coated with a second less noble metal with increasing shell thickness. Our results of Figure 4 and, to a lesser extent, of Figures 1a and 2 fairly agree with the calculated spectra for the system Au/Ag[26] (Ag less noble than Au), while the results of Figure 9 rather correspond to the spectra already calculated for the system Ag/Au[28,34] (Au in cyanide solutions less noble than Ag).

The surface plasmon bands of *intimately alloyed* clusters may as well be calculated according to Mie model, provided the data on real and imaginary parts of dielectric constants of the same alloy $Au_xAg_{1-x}$ would be available.

The wavelength-dependent absorbance $OD_\lambda$ in water of mono- or bimetallic clusters with a size much smaller than the wavelength of light is given by the dipolar term of the Mie series:

$$OD = \frac{18\pi VNl\epsilon_0^{3/2}}{2.303\lambda} \frac{\epsilon_2}{(\epsilon_1 + 2\epsilon_0)^2 + \epsilon_2^2} \qquad (5)$$

where $\lambda$ is the wavelength in the vacuum, $l$ is the optical path, $V$ is the volume, $N$ is the number per volume unit of the particles, $\epsilon_0$ is the water permittivity, and $\epsilon_1$ and $\epsilon_2$ are the real and imaginary parts of the metal dielectric constant and depend both on $\lambda$. The absorbance maximum in the spectrum at the plasmon resonance $\lambda_{max}$ occurs when $\epsilon_1 = -2\epsilon_0$ (with $\epsilon_2 \ll 1$).

Since the cluster size controls the mean free path of the conduction electrons, the dielectric constants must take into account the size effects. Actually, it has been shown for monometallic clusters that the applicability of the model strongly depends on the accuracy of values of the dielectric constants involved.[28] The dielectric data we have used for bimetallic $Au_xAg_{1-x}$ clusters are known as a function of $x$.[44] We used for calculations of the spectrum for monometallic clusters the dielectric constants derived by Johnston and Christy.[45] The size effects were taken into account according to the method used by Kreibig:[46]

$$\epsilon_2(r) = \epsilon_2(\text{bulk}) + \frac{\omega_p^2 v_F}{\omega^3 r} \qquad (6)$$

where $r$ is the cluster radius, $\omega = 2\pi c/\lambda$ is the frequency, $\omega_p = 2\pi c/\lambda_p$ is the plasmon frequency for the bulk metal, and $v_F$ is the Fermi velocity. This equation is interpreted as the limitation of the mean free path of the electron by the particle dimension.

The same size correction ( eq 6) could be applied to alloyed clusters provided $v_F$ and $\omega_p$ values of the alloyed bulk metal would be available. Since $\omega_p$ values for pure Au ($1.38 \times 10^{16}$ $s^{-1}$)[47] and Ag ($1.35 \times 10^{16}$ $s^{-1}$)[47] are very close, the alloy frequency must also be not much different. The $v_F$ value is identical for Au and Ag ($1.4 \times 10^6$ m $s^{-1}$)[47] and is also adopted for the alloy.

Surface plasmon spectra for the various values of $x$ for which optical data are available[45] have been calculated. Only one maximum is found, in contrast with the spectra of core/shell clusters. The dependences on $x$ of calculated values of $\lambda_{max}$ and $\epsilon_{max}$ are presented in parts a and b of Figure 8 and compared with the corresponding experimental data. It is shown that the calculated figures are in excellent agreement with that determined experimentally. Similar calculations have been done by Mulvaney[34] for the alloy $Ag_{1-x}Au_x$. However, this author did not include the mean free path effects that somewhat affect the maximum position and mostly the extinction coefficient.

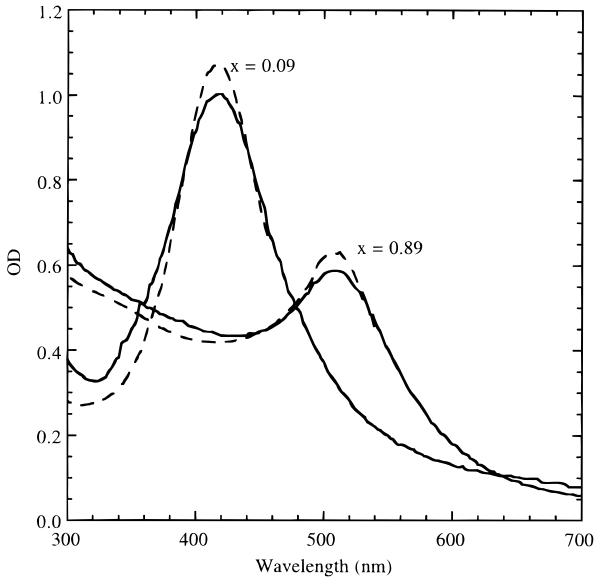


**Figure 11.** Plasmon spectra of spherical, homodispersed bimetallic alloyed Ag−Au (91/9), and (11/89) aggregates without interaction ($\phi$ 2.5 nm) calculated according to Mie theory, compared with the experimental spectra of Au−Ag bimetallic aggregates synthesized at a dose rate of 7.9 MGy $h^{-1}$: $[Au^{III}] + [Ag^I] = 10^{-3}$ mol $L^{-1}$, PVA = 0.1 mol $L^{-1}$, [2-PrOH] = 0.2 mol $L^{-1}$, dose = 20 kGy.

Calculated surface plasmon spectra obtained for alloyed $Ag_{1-x}Au_x$ clusters with $x = 0.09$ and 0.89 and a mean radius $r$ = 2.5 nm are presented in Figure 11, together with the corresponding experimental spectra. The shapes of the spectra, experimental and calculated, are quite similar. The position and the intensity of the maximum agree as shown in Figure 8 for various $x$ values.

Concerning the dependence of $\lambda_{max}$ on $x$, we may consider[16] that the surface plasmon frequency $\omega_{sp} = 2\pi c/\lambda_{max}$ of clusters is proportional to the plasmon frequency of the bulk metal $\omega_p$:[48]

$$\omega_p^2 = \frac{n_e e^2}{m^*} \qquad (7)$$

where $n_e$ is the electron density, $e$ is the electron charge, and $m^*$ is the effective mass. We also consider that the electron density of an alloyed cluster depends on the metal composition:

$$n_{e,alloy} = x n_{e,Au} + (1 - x) n_{e,Ag} \qquad (8)$$

Since the effective mass is almost the same for Ag and Au,[45] the variation of $\lambda_{max}(x)$ with $x$ of the alloy $Au_xAg_{1-x}$ is well described by

$$\lambda_{max}(x) = \frac{1}{\sqrt{\frac{x}{\lambda_{max,Au}^2} + \frac{1-x}{\lambda_{max,Ag}^2}}} \qquad (9)$$

Note that the variation of $\lambda_{max}(x)$ according to eq 9 is also in fair agreement with the experimental data and with the values calculated from optical data[44] (Figure 8a). In contrast with the curve derived from eq 9 for $Ag_xPd_{1-x}$,[16] the curve for $Ag_xAu_{1-x}$ is not far from linearity, as shown also by results obtained[49] for clusters prepared by evaporation of an alloyed electrode of AgAu through electric discharge and condensation into 2-butanol.

Note that it is difficult to conclude whether the structure of clusters known to contain two different metals is alloyed or is a core/shell from only their final absorption spectrum after complete reduction because in both cases the spectra are between those of pure metal clusters. The alloyed character must be assessed, as we have shown, on other arguments such as an unchanged spectrum with reduction of the mixed ion solution or an independent structure characterization.

**Mechanism.** *Nucleation and Growth of Bimetallic Alloyed Clusters*. The synthesis of bimetallic alloyed clusters, as in solid solutions, and especially of perfectly ordered aggregates implies a progressive reduction of the ions according to their abundance in solution. As already pointed out to explain the formation of bimetallic clusters[3,7,9,18,39] mostly for metals of very distinct redox properties, these results imply the preponderant influence of kinetics before electrochemical equilibrium between a noble and a less noble metal could be established. A perfect order obviously implies an intimate mixing of atoms from the very early steps of aggregation.

First, metal ions are reduced by radiolytic species according to reactions 3 and 4 and with the value of the reduction yield $G_{red} = 6$ equiv/100 eV, which means that solvated electrons and alcohol radicals are totally scavenged by metal ions:

$$e^-_{aq} + Ag^+ \rightarrow Ag^0 \quad (10)$$

$$e^-_{aq} + Au^{III} \rightarrow Au^{II} \quad (11)$$

$$(CH_3)_2C^{\bullet}OH + Au^{III} \rightarrow (CH_3)_2CO + Au^{II} + H^+ \quad (12)$$

Then the divalent gold ions disproportionate:[50,51]

$$Au^{II} + Au^{II} \rightarrow Au^{III} + Au^{I} \quad (13)$$

Finally monovalent gold ions disproportionate and are also reduced:

$$e^-_{aq} + Au^{I} \rightarrow Au^0 \quad (14)$$

Particularly important are the reactions of mixed association between reduced atoms or clusters and excess ions. Association between atoms and ions, homologous or different, may rapidly occur as observed in monometallic systems:

$$Ag^0 + Ag^+ \rightarrow (Ag_2)^+ \quad (15)$$

$$Au^0 + Au^{I} \rightarrow (Au_2)^+ \quad (16)$$

$$Ag^0 + Au^{I} \rightarrow (AuAg)^+ \quad (17)$$

$$Au^0 + Ag^+ \rightarrow (AuAg)^+ \quad (18)$$

Note that the mixed associations of reactions 17 and 18 lead to the same bimetallic complex. Recent data obtained by pulse radiolysis have shown that the mixed association is a very general process, often followed by electron transfer.[37,41]

Further coalescence of the primary bimetallic complexed species keeps the metals alloyed:

$$(AuAg)^+ + (AuAg)^+ \rightarrow (AuAg)_2^{2+} \quad (19)$$

Alternate association of primary mono- or bimetallic complexed species formed by reactions 15−18 with surrounding ions of both types and reduction of these ions enhance as well the probability of alloying the metals. Once reduced, bimetallic clusters of increasing size are thus formed:

$$(Au_mAg_n)^{x+} + Au^+ \rightarrow (Au_{m+1}Ag_n)^{(x+1)+} \quad (20)$$

$$(Au_{m+1}Ag_n)^{(x+1)+} + e^-_{aq}\ (\text{or}\ (CH_3)_2C^{\bullet}OH) \rightarrow (Au_{m+1}Ag_n)^{x+}\ (+(CH_3)_2CO + H^+) \quad (21)$$

Subsequent reductions such as reaction 21, and associations such as reaction 20, according to the statistics of encounters (i.e. to the initial ionic ratio), would result in the progressive building of an intimate solid solution with a composition similar to the composition of the initial precursor solution. Note that such an alloying of the Ag and Au process is observed for the first time by means of a radiolytic reduction of ionic precursors provided the dose rate is high enough, whereas by chemical reduction bilayered clusters were found.[21, 25]

*Intermetal Electron Transfer*. Under certain conditions of low dose rate, the overall reduction of mixed solutions seems to concern gold first, silver being reduced in a second step, although in monometallic solutions of each ion the initial reduction rates are the same. In fact, we must consider that the initial probabilities of being reduced by radiolytic species are almost identical for both metal ions (reactions 6−12), but in further steps electron transfer from silver atoms toward adsorbed gold ions systematically favors the gold reduction at the expense of silver during the irradiation. This eventually causes metal segregation across the cluster depth. When gold ions are almost exhausted, silver reduction on gold clusters may occur. The observed preferential reduction of gold under conditions of low dose rate implies that silver atoms and the smallest aggregates may systematically transfer electron to gold ions or that the redox potential of bimetallic clusters is systematically higher when a silver atom is replaced by a gold atom. Therefore, in these systems intermetallic electron transfer takes place in competition with the mechanism containing reactions 15−21:

$$(AuAg)^+ + Au^{I} \rightarrow (Au_2Ag)^{2+} \rightarrow (Au_2)^+ + Ag^+ \quad (22)$$

$$\text{result:}\quad (Au_mAg_n)^{x+} + Au^{I} \rightarrow (Au_{m+1}Ag_n)^{(x+1)+} \rightarrow (Au_{m+1}Ag_{n-1})^{x+} + Ag^+ \quad (23)$$

Another gold ion may again displace another silver atom so that the cluster contains essentially pure reduced gold. The absolute potential values of bimetallic clusters are unknown. However, it is worth noting that bulk gold in the presence of $Cl^-$ is also more noble than bulk silver. The irreversibility of the electron transfer lies in the second part of reaction 22 or 23 with the release of the less noble ion (here, $Ag^+$). This monomolecular release reaction is in direct competition with the subsequent reduction of the addition complex as in reaction 21 which is controlled by the generation rate of radiolytic species, i.e., by the dose rate. When the complete reduction of ions is faster than eq 23, the bimetallic alloy is obtained (dose rates higher than 35 kGy $h^{-1}$). In contrast, at lower dose rates, the displacement of Ag by Au ions (reaction 23) becomes efficient and a bilayered intermetallic cluster is observed.

Electrochemical displacement of metal atoms from clusters by ions of a more noble metal is thermodynamically allowed. However, the process is too slow to compete with the mechanism containing reactions 1−3 and 8−12 when the latter is induced in a sudden far-from-equilibrium reduction through pulse irradiation.

*Application to Synthesis of Bimetallic Bilayered and Alloyed Clusters*. Composite clusters, alloyed or bilayered, are of prominent interest as catalysts. The above conclusions may therefore constitute a guide for selecting the conditions of the synthesis of composite metal clusters containing M and M′ in variable proportions, with either an alloyed or a core/shell structure. Actually, when bilayered clusters are desired with M in the core and M′, less noble than M, in the shell (note that this order may be reversed by the proper choice of ion complexation), radiation-induced reduction of the ion mixture must be achieved at low dose rate to allow the equilibrium of the displacement of M′ by $M^+$ to be reached:

$$e^-_{aq} + M^+ \rightarrow M \qquad (10')$$

$$e^-_{aq} + M'^+ \rightarrow M' \qquad (11')$$

$$M' + M^+ \rightarrow (MM')^+ \rightarrow M + M'^+ \qquad (17')$$

$$\text{result:} \quad (M_m M'_n)^{x+} + M^+ \rightarrow (M_{m+1} M'_n)^{(x+1)+} \rightarrow (M_{m+1} M'_{n-1})^{x+} + M'^+ \qquad (23')$$

The result is a core−shell cluster where the less noble metal M′ is coating M. The radiolytic reduction may also be applied successively in a two-step process, first to pure $M^+$ solution and then to a $M'^+$ solution containing $M_n$ nuclei. The same phenomenon is also to be expected any time a chemical reduction is slower that the intermetal electron-transfer process because the mixing step itself of the reactants is slow or because the reducing character of the reductant is weaker than that of $e^-_{aq}$.

The synthesis of alloyed clusters containing two (or even more) metals of quite different redox properties may be achieved at a high dose rate of a pulsed electron beam according to the observations on gold−silver alloyed clusters. A second condition is that the total dose absorbed allows the complete reduction of all ions in order to prevent a possible postirradiation displacement by residual ions. In fact, the method has been extended successfully[52] to other couples that exhibit improved catalytic efficiency in photographic processes and that could not yet be prepared through chemical reduction or $\gamma$ irradiation because at low dose rate the intermetal electron transfer was faster than the reduction rate. The initial reduction in reaction 10′ or 11′ is followed by association of atoms with ions as in reaction 17′. Then alternate association (reaction 20′) and reduction reactions (reaction 21′) progressively build bimetallic alloyed clusters:

$$(M_m M'_n)^{x+} + M^+ \rightarrow (M_{m+1} M'_n)^{(x+1)+} \qquad (20')$$

$$(M_{m+1} M'_n)^{(x+1)+} + e^-_{aq} \rightarrow (M_{m+1} M'_n)^{x+} \qquad (21')$$

The high dose rate delivered by electron beams (or by pulsed lasers for photochemical reductions) allows efficient competition in favor of reduction, thus preventing a possible intermetallic electron exchange that would cause metal segregation (reaction 23′). The required reduction, achieved within an extremely short time, shorter than in any other chemical or electrochemical process, may be compared with a sudden nonequilibrium quenching of atoms in the lattice and results in the building of an intimately alloyed cluster with the same metal ratio as for the ionic precursors. Note that when the precursors are multivalent ions, electron transfers are also possible between the lower valencies of both metals, therefore increasing the probability of a segregation, if the complete reduction is not fast enough. Interesting enough is that the dose rate required to ensure the alloying depends on the couple of metals and on the environment. Some alloys are formed at low dose rates of $\gamma$ sources such as Cu−Pd[7,8] and AgPd,[16] which means that the displacement is not efficient in the range of hours. In the case of Ag−Au in a $Cl^-$ environment the complete reduction has to be achieved within about 10 min for alloy formation and in $CN^-$ solutions within 2 s.[41]

The control of the intermetallic electron transfer even allows us to synthesize composite clusters where the *less* noble metal constitutes the core. After their reduction in the monometallic solution, the clusters $M'_n$ are mixed with a solution of $M^+$, then immediately submitted to a very intense and fast irradiation within a time much shorter than the reaction time of the electron exchange (Figure 10). At complete reduction, no more exchange may occur and the bilayered clusters are stable.

## Conclusion

Generally, the bimetallic character of several clusters synthesized by reduction of mixed solutions of ions is shown mostly indirectly through their exceptional catalytic efficiency. Few examples have been characterized directly by the use of microanalysis. In most of these systems, a segregation occurs during the reduction so that the more noble of the metals constitute the core and the less noble metal the shell of a bilayered cluster. This structure stems from an intermetallic electron transfer occurring with mixture reduction according to the respective redox potentials of the two metals. Initially, the reduction may be equiprobable but then the less noble atoms behave as electron relays toward the other metal ions up to the complete reduction of the latter, thus favoring the formation of clusters of the more noble metal first. The few exceptions observed of intimately alloyed metal clusters prepared either by chemical reduction or by low dose rate irradiation result from an extremely slow electron transfer, which allows the simultaneous reduction of both ions to occur under nonequilibrium kinetics.

The results presented here on the dose evolution of the surface plasmon spectra of mixed ion solutions progressively reduced allow us to make a clear discrimination between composite bilayered clusters and bimetallic intimately alloyed clusters of gold and silver. In some cases, independent structural data confirmed the alloyed character assessed on the dose evolution of the optical spectra. Their comparison with calculated spectra also seems to confirm the model reliability for alloyed clusters. If this kind of agreement could be confirmed as a general conclusion by similar comparisons extended to other systems, even unknown optical properties of alloyed metals could be derived from surface plasmon data of the clusters as proposed by Quinten.[46b] The use of the radiation-induced synthesis allowed us to tightly control the reduction rate through the dose rate conditions and thus to demonstrate its influence on the successive or simultaneous formation of the two types of metal atoms. Actually, the metal clusters obtained in the same mixed system change from a bilayered core/shell structure to a bimetallic solid solution with an increase of the dose rate. If the intermetallic electron transfer is quite fast, which seems to be the most frequent situation, only an extremely fast, total reduction through the use of pulse techniques is able to prevent any metal displacement and thus any segregation. All ions are suddenly reduced before an electron transfer may occur, and the atoms are quenched in a nanocrystal lattice, which reproduces the ratio of the precursors. This approach allows the

synthesis at room temperature of new kinds of bimetallic and even multimetallic alloyed clusters with a metal ratio close to that of the ionic precursors. Besides, it turns out that the method of radiation-induced reduction at the very high dose rate of an electron pulse yields mono- and bimetallic clusters of better homodispersity and markedly smaller size.

**Acknowledgment.** The authors are gratefully indebted to AGFA-GEVAERT Company for financial support, to Dr. V. Favaudon (Institut Curie, Orsay) for having given us access to the $\gamma$-irradiation facility, and to both C. Vignaud (Physique des Liquides & Électrochimie, Paris VI) and P. Beaunier (Groupement Régional de Mesures Physiques, Paris VI) for their contribution in characterization experiments through electron microscopy and diffraction or X-ray analysis.

## References and Notes

(1) Belloni, J.; Delcourt, M. O.; Leclere, C. *Nouv. J. Chim.* **1982**, *6*, 507.
(2) Henglein, A. *Chem. Rev.* **1989**, *89*, 1861; *J. Phys. Chem.* **1993**, *97*, 5457 and references therein.
(3) Belloni, J.; Amblard, J.; Marignier, J. L.; Mostafavi, M. In *Clusters of Atoms and Molecules II*; Haberland, H., Ed.; Chemical Physics 56; Springer: New York, 1994; p 291.
(4) Belloni, J. *Curr. Opin. Colloid Interface Sci.* **1996**, *1*, 184.
(5) (a) Delcourt, M. O.; Keghouche, N.; Belloni, J. *Nouv. J. Chim.* **1983**, *7*, 131. (b) Belloni, J.; Lecheheb, A. *Radiat. Phys. Chem.* **1987**, *29*, 89.
(6) (a) Bruneaux, J.; Cachet, H.; Froment, M.; Amblard, J.; Belloni, J.; Mostafavi, M. *Electrochem. Acta* **1987**, *32*, 1533. (b) Amblard, J.; Platzer, O.; Belloni, J. *J. Chim. Phys*. **1991**, *88*, 835.
(7) Marignier, J. L.; Belloni, J.; Delcourt, M. O.; Chevalier, J. P. *Nature* **1985**, *317*, 344.
(8) Belloni, J.; Marignier, J. L.; Delcourt, M. O.; Minana, M. U.S. Patent 4,629,709, December 16, 1986.
(9) Marignier, J. L. Thèse de Doctorat d'Etat, Université Paris-Sud, Orsay, 1987.
(10) Le Gratiet, B.; Remita, H.; Picq, G.; Delcourt, M. O. *J. Catal.* **1996**, *164*, 36.
(11) Georgopoulos, M.; Delcourt, M. O. *New J. Chem*. **1989**, *13*, 519.
(12) Sinfelt, J. H. *Acc. Chem. Res*. **1987**, *20*, 134.
(13) Bradley, J. S. In *Clusters and Colloids*; Schmid, G., Ed.; Weinheim: New York, 1994; p 459.
(14) Henglein, A.; Giersig, M. *J. Phys. Chem.* **1994**, *98*, 6931.
(15) Remita, S.; Mostafavi, M.; Delcourt, M. O. *Radiat. Phys. Chem.* **1996**, *47*, 275.
(16) Remita, H.; Khatouri, J.; Treguer, M.; Amblard, J.; Belloni, J. *Z. Phys. D: At., Mol. Clusters* **1997**, *40*, 127.
(17) Torigoe, K.; Nakajima, Y.; Esumi, K. *J. Phys. Chem.* **1993**, *97*, 8304.
(18) Belloni, J.; Delcourt, M. O.; Marignier, J. L.; Amblard, J. In *Radiation Chemistry*; Hedwig, P., Nyikos, L., Schiller, R., Eds.; Akademià Kiadò: Budapest, 1987; p 89.
(19) Sosebee, T.; Giersig, M.; Holzwarth, A.; Mulvaney, P. *Ber. Bunsen-Ges. Phys. Chem.* **1995**, *99*, 40.
(20) Mostafavi, M.; Remita S.; Picq G. To be published.
(21) Sato, T.; Kuroda, S.; Takami, A.; Yonezawa, Y.; Hada, H. *Appl. Organomet. Chem.* **1991**, *5*, 261.
(22) Yonezawa, T.; Toshima, N. *J. Chem. Soc., Faraday Trans*. **1995**, *91*, 4111.
(23) Yala, F.; Delarue, E.; Delcourt, M. O.; Haut, C.; Severac, C.; Grattepain, C. *J. Mater. Sci.* **1995**, *30*, 1203.
(24) Torigoe, K.; Esumi, K. *Langmuir* **1993**, *9*, 1664.
(25) Liz-Marzan, L. M.; Philipse, A. P *J. Phys. Chem.* **1995**, *99*, 15120.
(26) Morriss, R. H.; Collins, L. F. *J. Chem. Phys.* **1964**, *41*, 3357.
(27) Buxton, G.; Rhodes, T.; Sellers, R. *J. Chem. Soc., Faraday Trans 1* **1982**, *78*, 3341.
(28) Mulvaney, P.; Giersig, M.; Henglein, A. *J. Phys. Chem.* **1993**, *97*, 7061.
(29) Henglein, A.; Mulvaney, P.; Holzwarth, A.; Sosebee, T.; Fojtik, A. *Ber. Bunsen-Ges. Phys. Chem.* **1992**, *96*, 754.
(30) Henglein, A.; Mulvaney, P.; Linnert, T.; Holzwarth, A. *J. Phys. Chem.* **1992**, *96*, 2411.
(31) Mulvaney, P.; Giersig, M.; Henglein, A. *J. Phys. Chem.* **1992**, *96*, 10419.
(32) Henglein, F.; Henglein, A.; Mulvaney, P. *Ber. Bunsen-Ges. Phys. Chem.* **1994**, *98*, 180.
(33) Michaelis, M.; Henglein, A.; Mulvaney, P. *J. Phys. Chem.* **1994**, *98*, 6212.
(34) Mulvaney, P. *Langmuir* **1996**, *12*, 788.
(35) Henglein, A.; Tausch-Treml, R. *J. Colloid Interface Sci.* **1981**, *80*, 84.
(36) Mostafavi, M.; Marignier, J. L.; Amblard, J.; Belloni, J. *Radiat. Phys. Chem.* **1989**, *34*, 605.
(37) Ershov, B. G.; Janata, E.; Henglein, A. *J. Phys. Chem*. **1994**, *98*, 7619; *J. Phys. Chem.* **1994**, *98*, 10891.
(38) Ershov, B. G.; Janata, E.; Henglein, A. *Radiat. Phys. Chem.* **1996**, *47*, 59.
(39) Khatouri, J.; Mostafavi, M.; Amblard, J.; Belloni, J. *Chem. Phys. Lett.* **1992**, *191*, 351.
(40) Marignier, J. L.; Belloni, J. *J. Chim. Phys.* **1988**, *85*, 21.
(41) de Cointet, C.; Khatouri, J.; Mostafavi, M.; Belloni, J. *J. Phys. Chem. B* **1997**, *101*, 3517.
(42) Mie, G. *Ann. Phys*. **1908**, *25*, 377.
(43) Kreibig, U.; Vollmer, M. *Optical properties of metal clusters;* Springer: Berlin, 1995.
(44) Ripken, K. *Z. Phys.* **1972**, *250*, 228.
(45) Johnston, P. B.; Christy, R. W. *Phys. Rev. B* **1972**, *8*, 4370.
(46) (a) Sinzig, J.; Radtke, U.; Quinten, M.; Kreibig, U. *Z. Phys. D.* **1993**, *26*, 242. (b) Quinten, M. *Z. Phys. B* **1996,** *101*, 211.
(47) Alvarez, M. T.; Khoury, J. T.; Schaaff, T. G.; Shafigullin, M. N.; Vezmar, I.; Whetten, R. L. *J. Phys. Chem. B* **1997**, *101*, 3706.
(48) Halperin, W. P. *Rev. Mod. Phys*. **1986**, *58*, 533.
(49) Papavassiliou, G. C. *J. Phys. F: Met. Phys.* **1976**, *6*, L103.
(50) Ghosh-Mazumdar, A. S.; Hart, E. J. *Adv. Chem. Ser.* **1968**, *81*, 193.
(51) Baxendale, J. H.; Koulkès-Pujo, A. M. *J. Chim. Phys.* **1970**, *67*, 1602.
(52) De Keyzer, R.; de Cointet, C.; Treguer, M.; Remita, H.; Mostafavi, M.; Amblard, J.; Khatouri, J.; Belloni, J. AGFA Patent EP 95203 1706, November 20, 1995.